Water and the Environment
Pontifical Academy of Sciences, *Scripta Varia* 108, Vatican City 2007
www.pas.va/content/dam/accademia/pdf/sv108/sv108-rosenfeld.pdf

PRECIPITATION SUPPRESSION BY ANTHROPOGENIC AIR POLLUTION: MAJOR LOSS OF WATER RESOURCES WHERE WE NEED THEM MOST

DANIEL ROSENFELD

1. The Effect of Aerosols on Cloud Composition and Precipitation Forming Processes

Precipitation forms by coagulation of many small cloud particles into precipitation-size particles. The typical size of cloud drops is 10 μm, whereas the size of small raindrops is 1000 μm, or 1 mm. Therefore the mass of about one million cloud drops must be combined to form one rain drop. The rate of coagulation of cloud drops to precipitation critically depends on their size. At least some of the cloud drops must have a radius >15 μm for the effective formation of precipitation in that cloud.

The size of the cloud drops is determined to a large extent by the properties of the aerosols. Cloud drops nucleate on aerosol particles when the air cools and reaches super-saturation with respect to water vapor, similar to the way that dew forms on the surface of cool objects. Aerosols that contain some water soluble materials serve as good cloud condensation nuclei (CCN). Such are smoke and air pollution particles. Therefore, clouds that form in polluted air are composed of a larger number of smaller drops than similar clouds that form in pristine air. The size reduction of cloud drops slows down their coagulation and so acts to suppress the precipitation from polluted clouds. This principle has been known since the 1950s (Gun and Phillips, 1957). However, the extent and practical importance of the effects of air pollution on precipitation were not known until very recently, when space-borne measurements of cloud properties and precipitation became available. Here we will review the main findings achieved with these new capabilities.

The effect of pollution aerosols suppressing precipitation is best seen on the pristine background of marine layer clouds, when polluted by effluents from ship stacks (Rosenfeld *et al.*, 2006a) (see Figure 1, page 220).

2. Impacts of Urban and Industrial Air Pollution on Precipitation

Rosenfeld (2000) used both satellite remote sensing in the visible and IR, and measurements from the radar aboard the TRMM satellite, to examine how urban and industrial pollution might inhibit precipitation development. They illustrated that ship track-like features occur also over land. The showed such pollution tracks can be found in the Middle East, in Canada, and South Australia (see Figure 2, page 221). He inferred that the pollution tracks were clouds composed of numerous small droplets that inhibit precipitation formation. It is interesting to note that this effect is not limited to warm clouds. Some of the clouds exhibiting pollution tracks were in Canada, where ice precipitation processes are prevalent. Perhaps most significant in Rosenfeld's analysis is the conspicuous absence of pollution tracks over the United States and Western Europe, in a background of clouds that already have small effective radii (Rosenfeld and Woodley, 2003). Furthermore, the pollution tracks in Australia could be clearly identified as far as 1500 km inland, indicating that without anthropogenic aerosols the clouds remain pristine well inland, at least in this case. The implication is that these regions in the USA and Europe are so heavily polluted that clouds affected by local sources cannot be distinguished from the widespread pollution-induced narrow cloud droplet spectra in surrounding regions.

Figure 3a (see page 222) shows an image taken from TRMM over Australia in which a pollution plume affects clouds over a large distance. In Figure 3b (see page 222) the TRMM radar measurements show that the region affected by the polluting aerosols had no radar reflectivity (the minimum detectable signal was 17 dBZ, which corresponds to about 0.7 mm hr^{-1}), suggesting negligible rain. Figure 3c (see page 222) shows the effective drop radii at cloud tops in three regions (1, 2 and 3). The effective radius in region 2 never exceeded the precipitation threshold of 14 μm.

3. Impacts of Smoke From Burning Vegetation on Precipitation

Rosenfeld and Lensky (1998) retrieved cloud particle effective radius and temperature from satellite data for inferring that smoke from forest fires in Indonesia suppressed rain in the tropical clouds over Indonesia and Malaysia. These inferences were validated by cloud physics aircraft measurements over Indonesia (Rosenfeld and Lensky, 1998), as well as by spaceborne radar and passive microwave measurements (Rosenfeld, 1999). Rosenfeld (1999) used the Tropical Rainfall measuring Mission (TRMM) satellite measurements over Indonesia that showed clouds ingesting smoke were devoid of precipitation up to the −10°C isotherm, whereas nearby clouds in smoke free air developed significant warm rain (i.e., rain that forms without involvement of the ice phase). The TMI (TRMM Microwave Imager) detected a large amount of water in the smoky clouds, but the lack of detectable precipitation echoes by the TRMM radar meant that all this water remained in the form of cloud drops, which are too small to create radar echoes (see Figures 4-6, pages 223-224). Similar evidence for smoke suppressing warm rain processes in deep tropical convective clouds up to the −10°C isotherm were made using TRMM in clouds ingesting smoke over India (Rosenfeld *et al.*, 2002) and over the Amazon (Rosenfeld and Woodley, 2003). Aircraft measurements in smoky and smoke-free clouds validated these satellite inferences in both the Amazon and Thailand (Andreae *et al.*, 2004). Heavy smoke from burning oil wells showed similar impacts on the clouds (Rudich *et al.*, 2003). Very heavy smoke from fires was also observed to suppress precipitation, except for large hail, up to the anvil level (From *et al.*, 2006).

The importance of coalescence in the production of rainfall from tropical convective cells that were tracked by radar throughout their life cycle has been investigated by Rosenfeld and Woodley (2003) using volume-scan radar observations from the AARRP (Applied Atmospheric Research Resources Project) 10-cm, Doppler radar in northwest Thailand, where most of the aerosols were generated by agricultural fires. The radar estimates of the tracked cell properties were partitioned using in-situ observations of the presence or absence of detectable raindrops by the aircraft as it penetrated the updrafts of growing convective towers, 200 – 600 m below their tops at about the –8°C level (about 6.5 km MSL). Figure 7 (see over) shows that on conditions with suppressed coalescences negligible rainfall was produced by cells with echo tops <~5 km compared to the rainfall amounts from similar clouds that have active warm rain processes. The rainfall from the deepest clouds is greater by more than a factor of 100, but still the deep convective clouds with suppressed coalescence produce only about half the rainfall of similar clouds but with observed warm rain.

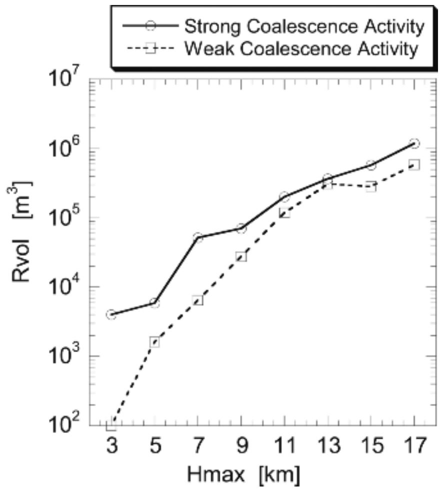

Figure 7. The mean rain volumes of convective cells as a function of maximum precipitation echo top height for cells growing on days with weak coalescence activity and on days with strong coalescence activity. The data are plotted at the center point of 2 km intervals of maximum echo top height. For the purpose of showing the trend on a logarithmic scale, a value of 10^2 m^3 was used instead of the zero value of RVOL for the 3 km maximum echo top height interval for cells growing on days with weak coalescence activity. From Rosenfeld and Woodley (2003).

4. Impacts of Pollution Aerosol on the Vigor of Deep Convective Clouds

Pollution aerosols have been documented to suppress precipitation from shallow clouds (cloud heights below about the −10°C isotherm) (Rosenfeld, 1999 and 2000, Phillips *et al.*, 2002, Albrecht, 1989, Rosenfeld *et al.*, 2002). When polluted clouds develop to greater heights (lower temperatures), however, as often happens in the summertime over land, D. Rosenfeld suggested (in Williams *et al.*, 2002 and Andreae *et al.*, 2004) that suppressed rainout enables unprecipitated water to reach greater heights, where freezing can release additional latent heat and further invigorate the cloud updrafts. This might in turn delay the onset of precipitation and the development of downdrafts and so prolong the growth of the convective cloud, allowing more water vapor to be ingested and further invigorate the storms (Andreae *et al.*, 2004). This conjecture is supported by the observations of Devasthale *et al.* (2005). They compared the AVHRR retrieved cloud top temperatures over central and Eastern Europe that saw radical infrastructural changes after the fall of the East Bloc in 1989 that has affected the pollution levels and hence cloud properties. Four years in the late 1980s (1985-1988) and in the late 1990s (1997-2000) were compared, as these are distinctively marked as episodes of very high and lower air pollution (sulfates and particulate matter). During the late 1980s, convective cloud tops were colder by 4 K. Devasthale *et al.* (2005) concluded that 'cloud-tops over and around polluted regions are higher, and their temperatures showed stronger variability, suggesting an indirect aerosol effect in the thermal spectral range as well'. This is also supported by satellite observations showing that clouds develop to greater heights in more polluted air masses (Koren *et al.*, 2005).

Cloud simulations (Khain *et al.*, 2005, Seifert and Beheng, 2006, Teller and Levin, 2006, Van Den Heever *et al.*, 2006) lend further support for the suggestion that pollution aerosols in moist unstable atmosphere can induce clouds to develop stronger updrafts and downdrafts, grow taller, trigger secondary storm development, and produce more rain.

5. Effects of Air Pollution on Orographic Clouds and Precipitation

Borys *et al.* (2000) and Borys *et al.* (2003) provided some evidence that pollution can suppress precipitation in winter orographic clouds in the Rocky Mountains. Their analysis shows that pollution increases the concentration of CCN and therefore cloud drops, leading to the formation of smaller cloud drops. The reduced drop size leads to less efficient riming and therefore to smaller ice crystals (Fig. 8, see over), smaller fall velocities, and less snowfall.

Borys *et al.'s* observation was supported by Givati and Rosenfeld (2004) who analyzed about 100 years of precipitation records in regions downwind of pollution sources and compared them to precipitation in regions unaffected by these sources. Givati and Rosenfeld (2004) documented the trends in the orographic enhancement factor, Ro, which is defined as the ratio between the precipitation over the hill with respect to the upwind lowland precipitation amount. Two geographical areas were chosen for this study: California and Israel. The topography in both regions is similar, although the mountains in Israel are much lower than the Sierra Nevada. The statistical results for both locations show that downwind of pollution sources, on the upslope of mountains and mountain tops, orographic precipitation is reduced by ~20% and ~7%, respectively (Figure 9, see page 225). It was hypothesized that this decrease is due to an increase in droplet concentrations and a decrease in droplet size. Farther downwind on the lee side of mountains, the amount of precipitation is increased by ~14%. The authors postulate that this increase is due to smaller cloud particles taking longer time to grow, allowing the winds aloft to carry them over the mountain top (see earlier study of similar effects, produced by deliberate over seeding with ice-producing particles, by Hobbs, 1975). However, the integrated rainfall amount over the whole mountain range appeared to be reduced by the pollution. The possible effects of moisture and low level winds were considered using a radiosonde regression model, which showed that the relevant meteorological conditions during rain days did not change systematically along the years, and the observed trends in the ratio of hill / plain precipitation are likely caused by non-meteorological reasons (Givati and Rosenfeld, 2004).

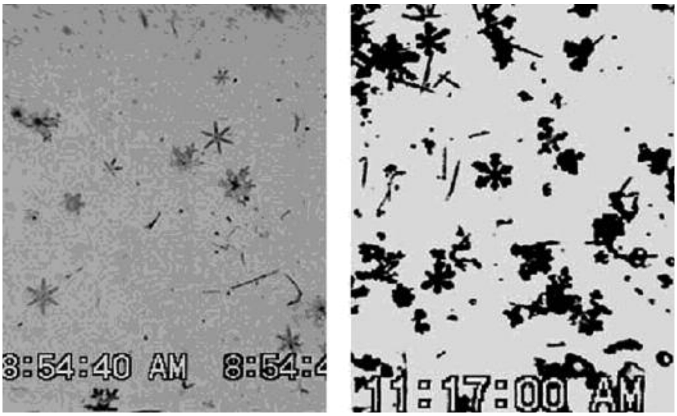

Figure 8. Light riming of ice crystals in clouds affected by pollution (left) compared to heavier riming in non-polluted clouds (right). From Borys *et al*. (2003).

Rosenfeld and Givati (2006) expanded this analysis to the whole western USA. The analyses of trends of the orographic winter precipitation enhancement factor, Ro, along the coastal mountain ranges of the west coast of the USA show a pattern of decreasing Ro during the last century by as much as −24% from the southern border to central California, to no decrease in northern California and Oregon, and to a renewed decrease of Ro (−14%) in Washington to the Seattle area east of Puget Sound. Similar decreases occurred also well inland, over Arizona, New Mexico, Utah

(Rosenfeld and Givati, 2006) and the east (already documented by Jirak and Cotton, 2006) slopes of the Colorado Rockies. Both absolute precipitation amounts and Ro are affected by fluctuations in the atmospheric circulation patterns such as those associated with the Pacific Decadal Oscillation and the Southern Oscillation Index. However, these climatic fluctuations can not explain the observed trends in Ro. Although the trends of aerosols are available only since 1988, aerosol measurements from the IMPROVE aerosol monitoring network show that negative trends in Ro are associated with elevated concentrations of fine aerosols (PM2.5). The PM2.5 showed stability or some increase in the areas where their levels were elevated and decreasing trends of Ro were noted. Strong decreasing trends of the coarse aerosols (PM10-PM2.5) were noted especially in the areas with elevated levels of PM2.5. The decreasing trend in coarse aerosols (the coarse aerosols may act to initiate and enhance precipitation) in conjunction with the constancy and/or increases of the small aerosols (small aerosols suppress precipitation), can explain the continuing losses of orographic precipitation during the last two decades despite the indicated improvement in the conventional air quality standards (Rosenfeld and Givati, 2006).

In line with these considerations, despite the reported decreases in the pollutant emissions in California during the last two decades, the total amount of soluble pollution ions in precipitation particles before falling below cloud base has not shown any decreasing trend and even showed a slight increasing trend in Sequoia National Park. Therefore, the expectation for a recent recovery of the orographic precipitation with the improving standards cannot be supported by these observations of the recent trend of steady to increasing concentrations of pollution in the precipitation. The concentrations of the pollution ions in the rainwater were only half the values in Lassen Volcanic National Park, where no decreasing trend of orographic precipitation was observed (Givati and Rosenfeld, 2004).

Evidence for the role of air pollution in suppressing precipitation in California was provided by in situ cloud physics aircraft measurements over central California during winter storms (Rosenfeld *et al.*, 2006d). They showed a clear maximum in the CCN concentrations downwind of San Francisco that were ingested into clouds and suppressed the coalescence and warm rain in them. In contrast, clouds in nearby sparsely populated areas remained maritime and with ample warm rain all the way to the Central Valley, where elevated CCN concentrations suppressed the warm rain from clouds that were formed at the foothills of the Sierra Nevada. The source of the CCN in populated areas was revealed as tracks of clouds with reduced effective radius emanating from the urban areas of San Francisco and the Central Valley.

Jirak and Cotton (2006) reached similar conclusions about the suppression of precipitation due to pollution on the Front Range of the Rocky Mountains. They report that the ratio of upslope precipitation for elevated sites west of Denver and Colorado Springs, Colorado to upwind urban sites has decreased by approximately 30% over the past half-century. Similar precipitation trends were not found for more pristine sites in the region.

These reported decreasing trends of the orographic precipitation were observed during the winter season. No decreasing trend was indicated in the amount of summer convective clouds over the hills (Rosenfeld and Givati, 2006). Furthermore, Diem and Brown (2003) partially attributed downwind summer convective precipitation enhancement in Phoenix to increased pollution-derived CCN, although they acknowledged that increased humidity from irrigation projects, and urban land-use induced surface convergence, were likely the dominant factors.

6. Impacts of Large Salt Particles on Enhancing Precipitation

Super-micron salt particles act as giant CCN that enhance precipitation, especially on the background of large concentrations of small CCN. The most common source of such particles is sea spray. Rosenfeld *et al.* (2002) suggested that clouds forming in polluted air over the ocean regain their precipitation ability mainly due to the added sea spray. They used the TRMM satellite and the in-situ measurement done in the INDOEX projects to document the evolution of aerosols and the related cloud microstructure and precipitation in the polluted air flowing off the Southeast Asia continent in the winter monsoon. Apparently raindrops initiated by the sea salt grow by collecting small cloud droplets that form on the pollution particles, thereby cleansing the air, as indicated by the gradual growth of the cloud drops farther away from land. Therefore, sea salt helps cleanse the atmosphere of the air pollution, via cloud processes.

An alternative explanation to these observations is updraft velocities over ocean are weaker than over land; therefore a smaller fraction of the aerosols is nucleated into cloud droplets. In addition, more time is available for the coalescence to progress and form warm precipitation. However, simulations of the impacts of sea spray on clouds with base updrafts of only

1 ms^{-1} were able to replicate most of the observed differences between polluted clouds over land and ocean. To neutralize completely the effect of sea versus land surface Rudich *et al.* (2002) compared clouds that ingested salt dust that was raised by the wind from the desiccated bed of the Aral Sea. The clouds in the salt storm developed much larger drops than clouds sidewind of the salt dust source and exceeded the precipitation threshold of 14 μm (see Figure 10, page 226). These results are consistent with the earlier observations of effluents of giant CCN from paper mills enhancing precipitation (Hindman *et al.*, 1977).

7. Conclusions

The recent development of Earth observations made it possible to quantify the impacts of natural and manmade aerosols on clouds and precipitation. We are still at the early stages of this important task. At this time we can already say the following:

1. Small pollution aerosols from smoke of burning vegetation, urban and industrial air pollution serve as good cloud condensation nuclei. When ingested into clouds, these aerosols reduce the cloud drop size and this in turn suppresses the precipitation forming processes within the clouds.
2. Precipitation can be completely shutoff in polluted clouds with tops warmer than −10°C.
3. Air pollution can substantially reduce precipitation from short living shallow clouds such as typically occur over topographical barriers in winter storms. Climatology of winter precipitation over hills downwind of pollution sources shows reductions of 10% to 25% of the seasonal precipitation. This was found to be the case in western USA and in Israel, which are both areas where water shortage is already a major problem.
4. Air pollution suppresses precipitation also in deep convective clouds in the tropics and summer mid-latitude. However, when the unprecipitated cloud water is carried to the high and cold parts of the cloud it freezes there and contributes to the invigoration of the cloud and enhancs the risk of hail and damaging winds.
5. Large salt aerosols were observed to have the opposite effects with respect to those caused by small pollution particles.

The precipitation losses appear to affect mainly densely populated areas with high demand for the water resources. Possible mitigation action obviously would be less pollution of small aerosols. Another method would be cloud seeding for rain enhancement, because clouds that are most susceptible to suppression by pollution aerosols would be also the most conducive to rain enhancement cloud seeding. This was shown to be the case in Israel (Givati and Rosenfeld, 2005), where air pollution and cloud seeding were documented to have similar and opposite effects on the precipitation over the Galilee Hills.

REFERENCES

Albrecht, B.A., Aerosols, cloud microphysics, and fractional cloudiness, *Science,* 245, 1227-1230, 1989.

Andreae, M.O., Rosenfeld, D., Artaxo, P., Costa, A.A., Frank, G.P., Longo, K.M., and Silva-Dias, M.A.F., Smoking rain clouds over the Amazon, *Science*, 303, 1337-1342, 2004.

Borys, R.D., Lowenthal, D.H., and Mitchel, D.L., The relationship among cloud physics, chemistry and precipitation rate in cold mountain clouds, *Atmos. Environ.*, 34, 2593-2602, 2000.

Borys, R.D., Lowenthal, D.H., Cohn, S.A., and Brown, W.O.J., Mountaintop and radar measurements of anthropogenic aerosol effects on snow growth and snow rate, *Geophys. Res. Lett.,* 30(10), 1538, doi: 10.1029/2002GL016855, 2003.

Devasthale, A. Kruger, O., Grassl, H, 2005: Change in cloud-top temperatures over Europe. Geoscience and Remote Sensing Letters, IEEE, 2, 333-336.

Diem, J.E., and Brown, D.P., Anthropogenic impacts on summer precipitation in central Arizona, U.S.A., *The Prof. Geograph.,* 55, 343-355, 2003.

Fromm M., Tupper, A., Rosenfeld D., Servranckx, R., McRae, R., 2006: Violent pyro-convective storm devastates Australia's capital and pollutes stratosphere. *Geophys. Res. Let*., 33, L05815, doi:10.1029/2005GL025161.

Givati, A., and Rosenfeld, D., Quantifying precipitation suppression due to air pollution, *J. Appl. Meteor.,* 43, 1038-1056, 2004.

Givati, A. and Rosenfeld, D., Separation between Cloud-Seeding and Air-Pollution Effects. *J.Appl. Meteor., 44,* 1298-1315, 2005.

Hindman, E.E. II, Hobbs, P.V., and Radke, L.F., Airborne investigations of aerosol particles from a paper mill, *J. Air Poll. Cont. Assoc.,* 27, 224-229, 1977.

Jirak, I.L., Cotton, W.R., Effect of Air Pollution on Precipitation along the Front Range of the Rocky Mountains, *J. Appl. Meteor. Climat.*, 45, 236-246, 2006.

Khain, A., Rosenfeld, D., and Pokrovsky, A., Aerosol impacts on the dynamics and microphysics convective clouds, *Quart. J. Roy. Meteorol. Soc.*, 131, doi:10.1256/qj.04.62, 2639-2663, 2005.

Koren I., Kaufman, Y.J., Rosenfeld, D., Remer, L.A., Rudich, Y., Aerosol invigoration and restructuring of Atlantic convective clouds, *Geophys. Res. Lett.,* 32, L14828, doi:10.1029/2005GL023187, 2005.

Gunn R. and Phillips, B.B., An experimental investigation of the effect of air pollution on the initiation of rain. *J. Meteor*., 14, 272-280, 1957.

Phillips, V.T.J., Choularton, T.W., Blyth, A.M., and Latham, J., The influence of aerosol concentrations on the glaciation and precipitation of a cumulus cloud, *Q. J. Roy. Meteor. Soc.*, 128(581), 951-971, 2002.

Rosenfeld D., and Lensky, I.M., Satellite-based insights into precipitation formation processes in continental and maritime convective clouds, *Bull. Amer. Meteor. Soc*., 79, 2457-2476, 1998.

Rosenfeld, D., TRMM observed first direct evidence of smoke from forest fires inhibiting rainfall, *Geophys. Res. Lett.*, 26, 3105-3108, 1999.

Rosenfeld, D., Suppression of rain and snow by urban and industrial air pollution, *Science,* 287, 1793-1796, 2000.

Rosenfeld, D., Lahav, R., Khain, A., and Pinsky, M., The role of sea spray in cleansing air pollution over ocean via cloud processes, *Science,* 297, 1667-1670, 2002.

Rosenfeld, D., and Woodley, W.L., Closing the 50-year circle: From cloud seeding to space and back to climate change through precipitation physics, *Meteor. Monogr.,* 51, 59-80, 2003.

Rosenfeld D., Givati, A, 2006: Evidence of orographic precipitation suppression by air pollution induced aerosols in the western U.S., *J. Applied Meteorology and Climatology*, 45, 893-911.

Rosenfeld D., Kaufman, Y., and Koren, I., 2006a: Switching cloud cover and dynamical regimes from open to closed Benard cells in response to aerosols suppressing precipitation. *Atmos. Chem. Phys.*, 6, 2503-2511.

Rosenfeld D., Woodley, W.L., Axisa, D., 2006b: Aircraft measurements of the impacts of pollution aerosols on clouds and precipitation over the Sierra Nevada. *12th Conference on Cloud Physics,* AMS, Madison, Wisconsin, 10-14 July 2006. Available at http://ams.confex.com/ams/pdfpapers/112407.pdf

Rudich, Y., Khersonsky, O., and Rosenfeld, D., Treating clouds with a grain of salt, *Geophys. Res. Lett.*, 29, 2060, doi:10.1029/2002GL016055, 2002.

Rudich Y., Sagi, A., Rosenfeld, D., Influence of the Kuwait oil fires plume (1991) on the microphysical development of clouds, *J. Geophys. Res*., 108, D15, 4478, doi:10.1029/2003JD003472, 2003.

Seifert, A. and Beheng, K.D., A two-moment cloud microphysics parameterization for mixed-phase clouds. Part II: Maritime vs. continental deep convective storms, *Meteorol. and Atmos. Phys.*, 92, 67-82, 2006b.

Teller, A. and Levin, Z., The effects of aerosols on precipitation and dimensions of subtropical clouds; a sensitivity study using a numerical cloud model, *Atmos. Chem. and Phys.*, 6, 67-80, 2006.

Williams, E., Rosenfeld, D., Madden M., *et al.*, 2002: Contrasting convective regimes over the Amazon: Implications for cloud electrification. *J. Geophys. Res.*, 107 (D20), 8082, doi:10.1029/2001JD000380.

Van Den Heever S.C., Carrió, G.G., Cotton, W.R., Demott, P.J., Prenni, A.J., Impacts of Nucleating Aerosol on Florida Storms. Part I: Mesoscale Simulations. *J. Atmos. Sci.*, 63, 1752-1775, 2006.

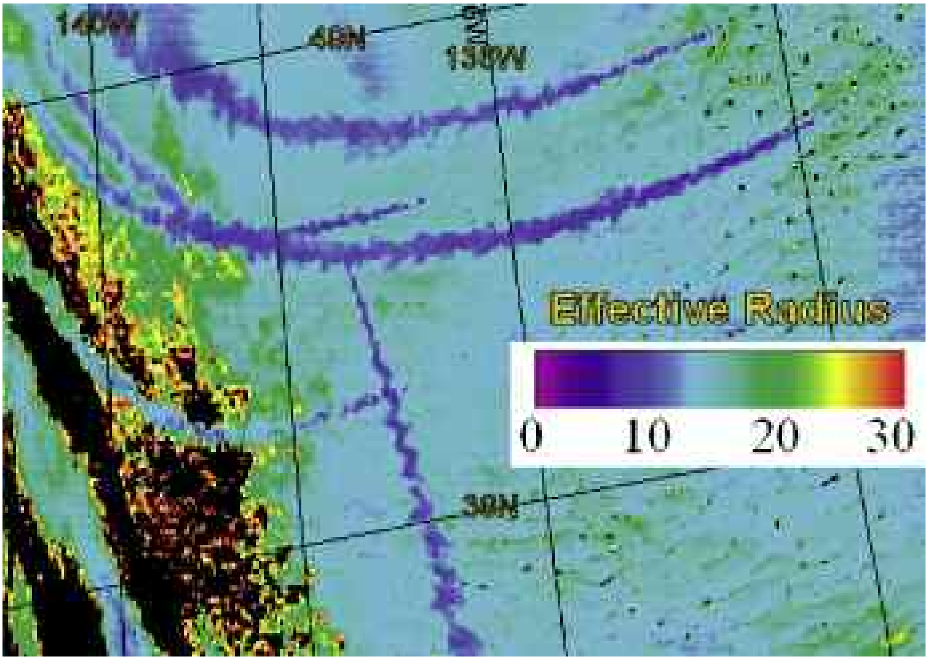

Figure 1: Ship tracks in marine layer clouds, manifested as linear features with reduced cloud drop effective radius. Clouds with effective radius > about 15 μm are partially dissipated due to loss of water by precipitation. The ship tracks are manifested as lines of solid cloud cover with small drops that prevent their dissipation by raining out. From Rosenfeld *et al*. (2006a).

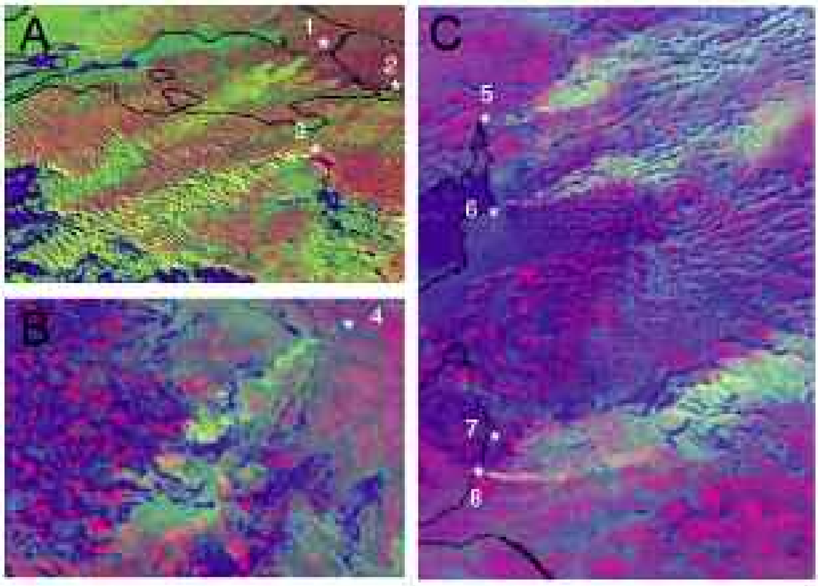

Figure 2. Satellite visualization of NOAA/AVHRR image, showing the microstructure of clouds with streaks of visibly smaller drops due to ingestion of pollution, originating from known pollution sources, marked by white numbered asterisks. The yellow streaks in panel A (about 300×200 km) originate from the urban air pollution of Istanbul (*1), Izmit (*2) and Bursa (*3), on 25 Dec 1998 12:43 UT. Panel B (about 150×100 km) shows the impact of the effluents from the Hudson Bay Mining and Smelting compound at Flin Flon (*4), Manitoba, Canada (54:46N 102:06W), on 4 June 1998 20:19 UT. Panel C (about 350×450 km) shows pollution tracks over South Australia on 12 Aug 1997, 05:26 UT, originating from Port Augusta power plant (*5), Port Pirie lead smelter (*6), Adelaide port (*7) and the oil refineries (*8). All images are oriented with north at the top. The images are color composites, where the red is modulated by the visible channel, blue by the thermal IR, and green is modulated by the solar reflectance component of the 3.7 μm channel, where larger (greener) reflectance means smaller droplets. That determines the color of the clouds, where red represents clouds with large drops, and yellow clouds with small drops. The blue background is the ground surface below the clouds. A full description of the color pallets and their meaning was provided by Rosenfeld and Lensky (1998). From Rosenfeld (2000).

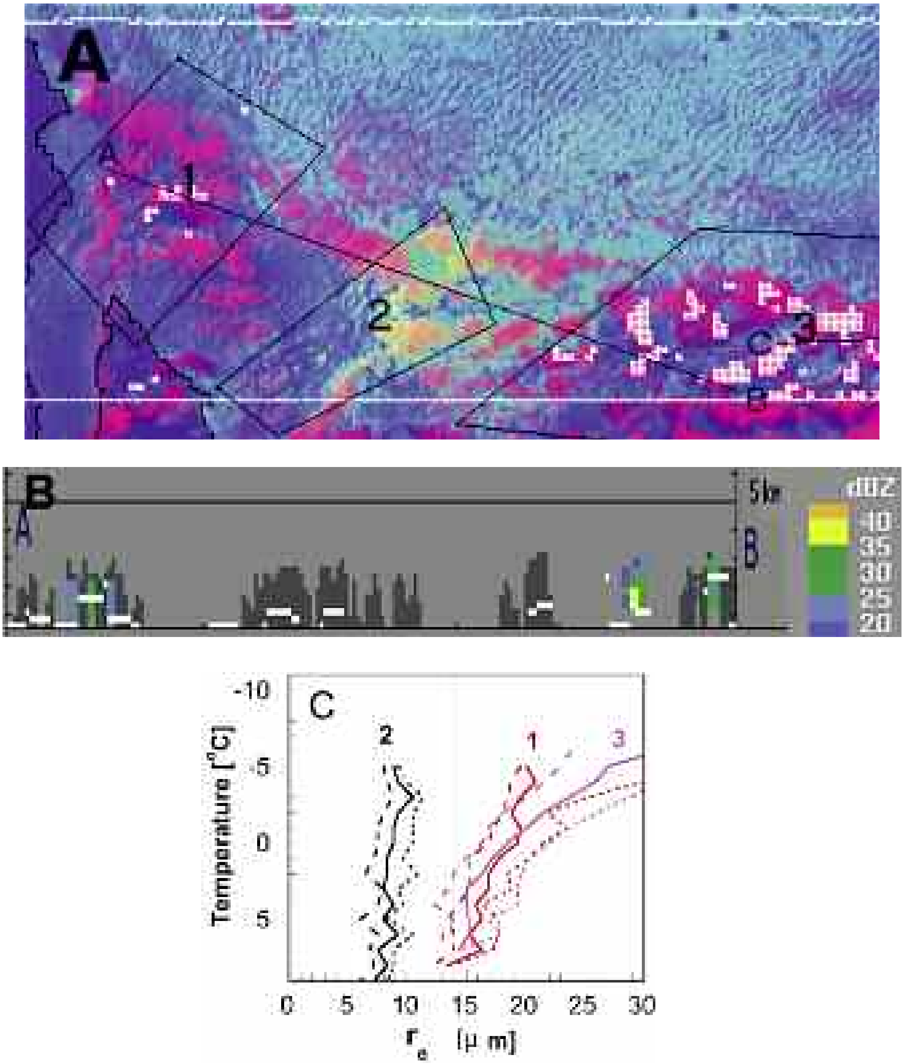

Figure 3 (a) Pollution tracks (yellow) detected by AVHRR satellite imagery in clouds over South Australia. The higher reflectivity is due to reduced droplet sizes. Radar shows precipitation as white patches outside pollution tracks, although these clouds have the same depth as adjacent non-polluted clouds, as shown in the vertical cross section (b). The gray clouds are the silhouettes obtained from the TRMM VIRS. The colors represent the radar echo intensities. No radar echoes occur within the clouds with reduced effective radius in Area 2. (c) Average effective radius of particles (probably water drops) at cloud tops in these regions (1, 2, and 3). The dashed lines represent the 15th and 85th percentiles of the distributions. From Rosenfeld (2000).

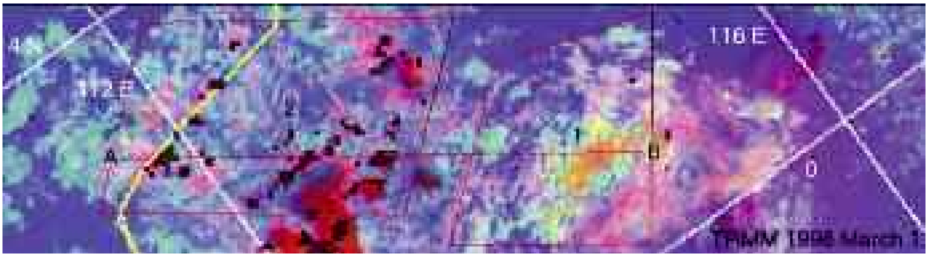

Figure 4. The TRMM VIRS image of fires, smoke and clouds over Kalimantan, Indonesia, from 1 March 1998, 02:50 UT. The color is composed of: red for visible reflectance, green for 3.7 mm reflectance (approximating the cloud drop effective radius, r_e), and blue for the inverse of 10.8 μm brightness temperature. The northwest coast of the island is denoted by the yellow line. The small orange areas on the upper right (east) corner are hot spots indicating the fires. The smoke, streaming from the hot spots south-westward, is indicated by the fuzzy purple color of the background. The smoke-free background is blue. This color scheme (see full detail in Rosenfeld and Lensky, 1998) shows clouds with small droplets (r_e<10 μm) as white, becoming yellow at the supercooled temperatures. Clouds with larger droplets (r_e>15 μm) are colored pink, and cold ice clouds appear red. The black hatching marks the areas in which the TRMM radar detected precipitation. From Rosenfeld (1999).

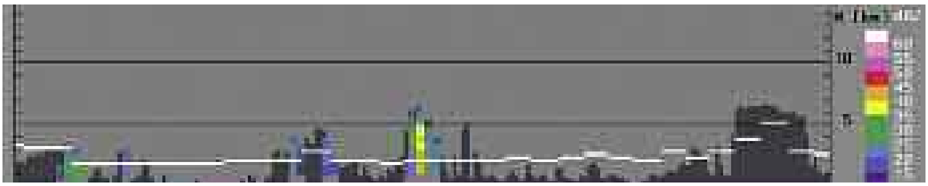

Figure 5. Vertical cross section along the line AB in Fig. 2, where the left end is point A and the right end correspond to point B in Fig. 2. The gray area is the clouds, as measured by their top temperature. The colors represent the precipitation reflectivity, in dBZ, as measured by the TRMM radar. The white line is the brightness temperature of the TRMM Microwave Imager 85 GHz vertical polarization, plotted at the altitude of that temperature. Please note that the 85 GHz brightness temperature and actual cloud top temperature have different physical meaning. From Rosenfeld (1999).

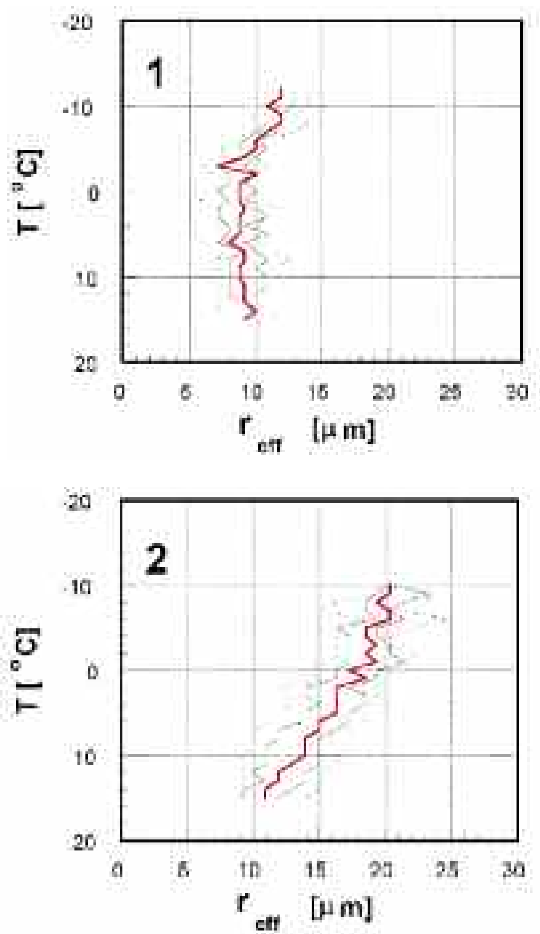

Figure 6. Analysis of the temperature (T) – droplet effective radius (r_e) relationship, for the clouds in the two boxes plotted in Fig. 4, respectively. Area 1 is smokey (on the right of Figure 4, whereas Area 2 is smoke-free. Plotted are the 10% 25% 50% 75% and 90% percentiles of the re for each 1°C interval. The median is indicated by the thick red line. From Rosenfeld (1999).

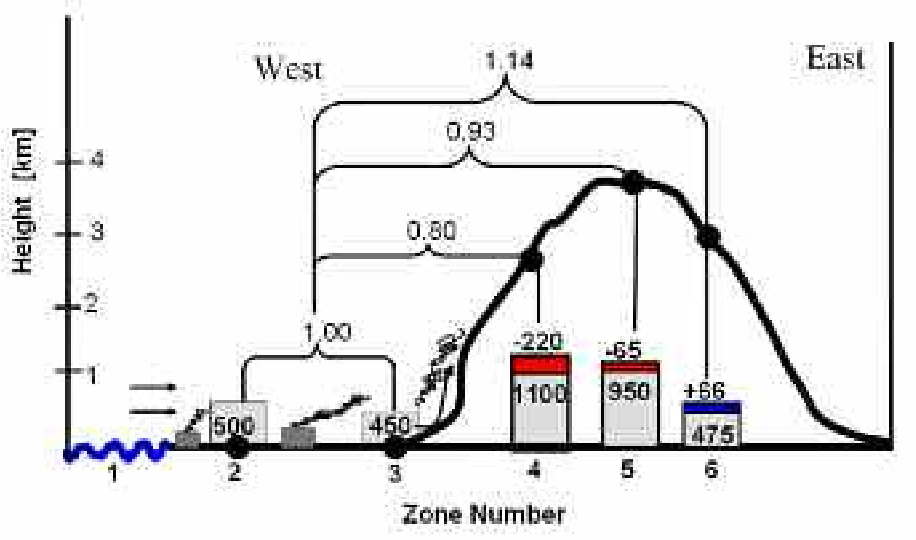

Figure 9. The effects of pollution on rainfall in the Sierra Nevada Mountains in California. The figure is a schematic topographic cross section showing the effects of urban air pollution on precipitation as the clouds move from west to east from the coast to the Sierra Nevada and to the eastern slopes. The boxes show the amount of the annual precipitation (mm yr^{-1}) in each topographic location, and the numbers above them show the loss or gain of precipitation (mm yr^{-1}) at each site. Maritime air (zone 1) is polluted over coastal urban areas (zones 2, 3), with no decrease in precipitation. The polluted air rises over mountains downwind and forms new polluted clouds (zone 4), with decreases of ~15%–20% (losses of 220 mm yr^{-1}) in the ratio between the western slopes and the coastal and plain areas (appears as 0.80 above the line connecting zones 4 and zones 2-3). The clouds reach to the high mountains in zone 5. All of the precipitation is snow, with a slight decrease of ~5%–7% (loss of 65 mm yr^{-1}) in the ratio between the summits and the plain areas (appears as 0.93). The clouds move to the high eastern slopes of the range (zone 6), with an increase of ~14% (gain of 66 mm yr^{-1}) in the ratio between the eastern slopes and the plain (appears as 1.14). From Givati and Rosenfeld (2004).

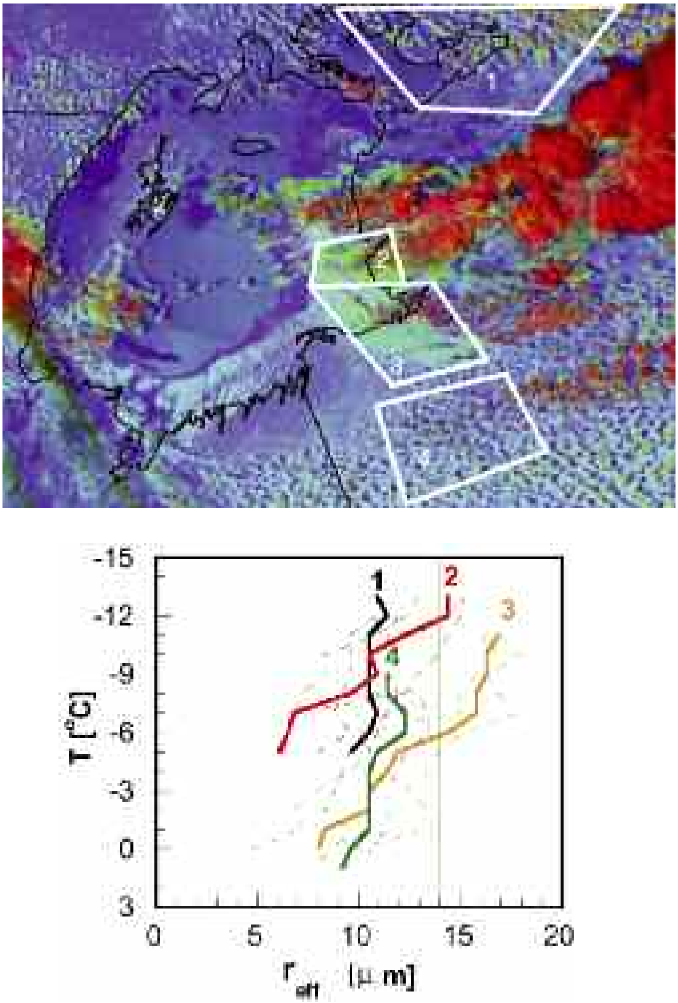

Figure 10. Left: NOAA – AVHRR satellite image (11 May 1998 09:32 UT) showing clouds forming in salt-dust plumes off the eastern shores of the Aral Sea (frames 2 and 3). Clouds outside the dust storm are shown in frames 1 and 4. Right: T-r_e relationship for the clouds in the 4 areas shown in the left panel. T is the temperature and r_e is the cloud particle effective radius. The solid lines show the median r_e for a given T, and the broken lines show the 15th and 85th percentiles. The vertical green line marks the 14-mm precipitation threshold. Curves 2 and 3 for clouds forming in heavy salt-dust show smaller near-cloud-base re and much larger cloud-top r_e compared to background clouds of comparable depths (curves 1 and 4). This analysis shows the fast growth of cloud droplets with height above cloud base. From Rudich *et al.*, (2002).